

A quantum walk approach to simulating parton showers

Khadeejah Bepari,^a Sarah Malik,^b Michael Spannowsky^a and Simon Williams^c

^a*Institute for Particle Physics Phenomenology, Department of Physics, Durham University, Durham DH1 3LE, U.K.*

^b*Department of Physics and Astronomy, University College London, Gower Street, London WC1E 6BT, UK*

^c*High Energy Physics Group, Blackett Laboratory, Imperial College, Prince Consort Road, London, SW7 2AZ, United Kingdom*

E-mail: khadeejah.bepari@durham.ac.uk, sarah.malik@ucl.ac.uk,
michael.spannowsky@durham.ac.uk, s.williams19@imperial.ac.uk

ABSTRACT: This paper presents a novel quantum walk approach to simulating parton showers on a quantum computer. We demonstrate that the quantum walk paradigm offers a natural and more efficient approach to simulating parton showers on quantum devices, with the emission probabilities implemented as the coin flip for the walker, and the particle emissions to either gluons or quark pairs corresponding to the movement of the walker in two dimensions. A quantum algorithm is proposed for a simplified, toy model of a 31-step, collinear parton shower, hence significantly increasing the number of steps of the parton shower that can be simulated compared to previous quantum algorithms. Furthermore, it scales efficiently: the number of possible shower steps increases exponentially with the number of qubits, and the circuit depth grows linearly with the number of steps. Reframing the parton shower in the context of a quantum walk therefore brings dramatic improvements, and is a step towards extending the current quantum algorithms to simulate more realistic parton showers.

Contents

1	Introduction	1
2	Quantum walks	2
3	Quantum walk as a parton shower simulation	3
3.1	Theoretical outline of shower algorithm	4
3.2	Implementation of a simple shower as a one-dimensional quantum walk	6
3.3	Implementation of a collinear parton shower	7
3.4	Towards a realistic parton shower	10
4	Summary	12

1 Introduction

The emergence of quantum computers has brought a new paradigm to the field of computation. The unique features of these devices has garnered attention from various disciplines, including High Energy Physics (HEP), where the computational challenges associated with taking, processing and analysing vast amounts of data in collider experiments like the Large Hadron Collider (LHC) requires innovative solutions. Quantum algorithms have been proposed to tackle some of these challenges, including the simulation of collision events [1–3] reconstruction of charged particle tracks in the detectors [4–6], and event classification and analysis [7–15].

Collision events at the LHC typically involve hundreds of particles and can be very complicated. Simulation of such events requires extensive modelling of proton-proton interactions and the subsequent detector response to fully uncover the underlying physics processes. Theoretical descriptions of these collisions can be separated into several stages. Constituent partons in the colliding protons can interact via large momentum transfer in the so-called hard interaction. Due to the large interaction energies, such collisions have the potential to probe new physics. Colour-charged particles produced as a result of this hard interaction are likely to emit further partons, resulting in a parton shower. The parton shower process evolves the system down in energy from the hard interaction to the hadronisation scale, $\mathcal{O}(\Lambda_{\text{QCD}})$. It is a perturbative process and can involve many partons, thus being one of the most time consuming parts of the generation of a collision event. Consequently, the development of quantum algorithms for the calculation of the hard process [2] and the resultant parton shower [1, 2] is an area of interest.

This paper presents a novel approach to simulating a many-particle, collinear parton shower on a quantum device using a quantum walk (QW) framework. It is structured as follows: Section 2 gives a brief introduction to the QW framework, Section 3 contains the

description of the proposed parton shower algorithm, and Section 4 gives a summary and conclusions.

2 Quantum walks

The quantum random walk [16–19] is the quantum analogue of the classical random walk and defines the movement of a particle, the *walker*, which can occupy certain *position* states on a graph. Here we will consider only discrete-time random walks, where a coin flip determines the movement of the walker at distinct time steps. The state of the walker can therefore be defined by the position of the walker, x , and the coin, c , as $|x, c\rangle$. The movement of the walker through the graph is determined by two operations: the coin operation, C , which determines the direction the walker will move, and the shift operation, S , which propagates the walker to the next position.

As a simple example, we construct a random walk following the approach in [18]. Consider a walker moving along a one-dimensional line according to an unbiased coin (i.e, the walker has an equal chance of moving left or right after the coin flip), with the walker originally positioned at $x = 0$, see Figure 1. The position of the particle on the line forms a Hilbert space \mathcal{H}_P spanned by integer values on the line, $\{|i\rangle : i \in \mathbb{Z}\}$. The position space is augmented by the coin-space, \mathcal{H}_C , which spans two basis states, $\{|\uparrow\rangle, |\downarrow\rangle\}$, the up and down spin-states of a fermion*. Therefore, the walker occupies a total space of

$$\mathcal{H} = \mathcal{H}_C \otimes \mathcal{H}_P. \quad (2.1)$$

In the classical case, the coin operation is carried out by evaluating a classical coin. Based on the outcome of this coin, the shift operator moves the walker in the correct direction. Here we will attribute the coin state $|\uparrow\rangle$ to the walker moving in the positive x direction and the $|\downarrow\rangle$ state to the walker moving in the negative x direction. After the step process is complete, the walker is either in the $x = -1$ or $x = 1$ position. In contrast to the classical case, the quantum coin operation is based on a *quantum coin*. In this example, we will consider the Hadamard coin,

$$H = \frac{1}{\sqrt{2}} \begin{pmatrix} 1 & 1 \\ 1 & -1 \end{pmatrix}, \quad (2.2)$$

which gives an equal chance for the coin to be measured in each of the coin states. The quantum coin operation puts the system into a superposition of the basis states of the \mathcal{H}_C space. The shift operation is then performed, moving the walker into a superposition of the position states, $x = -1$ and $x = 1$. A measurement after the step collapses the wavefunction to recover the classical case of the walker being in either the $x = -1$ or $x = 1$ position.

*The choice of using the up and down spin-states of a fermion is useful when implementing quantum walks on qubit-based quantum devices, such as those available on the IBM Q network [20].

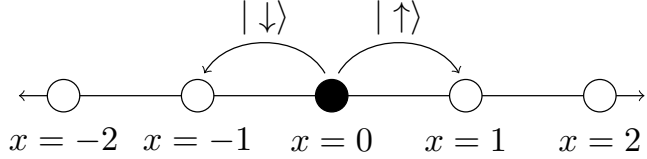


Figure 1: One-dimensional walker at position $x = 0$ can move either left or right depending on the outcome of the coin flip, $|\downarrow\rangle$ and $|\uparrow\rangle$ respectively.

The Hadamard coin used here is a balanced unitary coin operation[†] and therefore the coin and shift operations can be defined as a single unitary transformation to the initial qubit state,

$$U = S \cdot (C \otimes I), \quad (2.3)$$

which is applied iteratively to represent the number of steps. For a quantum walk of N steps, the propagation of the walker is described by the transformation U^N [18]. An example of running a linear, one-dimensional, $N = 100$ step, random walk for both the classical case and the quantum case is shown in Figure 2. The classical case has been achieved by measuring the *coin* qubit at each step, removing the superposition from the system. As expected, the classical walk yields a Gaussian distribution of positions centred about the initial position of the particle, with the variance $\sigma^2 = N$. In contrast, the quantum random walk, where the quantum interference between the intermediate steps of the walk process, results in a distribution that is dramatically different from the classical case. It can be shown [18, 21] that the variance of the quantum random walk process goes as $\sigma^2 \sim N^2$. This is a remarkable attribute of the quantum random walker, which propagates quadratically faster than the classical walker. The average distance of the walker from the initial position is $\sigma = \sqrt{N}$ and $\sigma \sim N$ for the classical and quantum walks, respectively.

3 Quantum walk as a parton shower simulation

The parton shower [23] evolves the energy scale of a scattering event from the hard interaction down to the hadronisation scale through the radiation of additional partons. The emissions are determined by splitting functions which correspond to the different emission probabilities in the shower. The shower content is then updated depending on which splitting probability is chosen. Due to this probabilistic interpretation of parton showers, the quantum walk mechanism provides a natural framework for the simulation of parton showers: the emission probabilities correspond to the coin flip probabilities, and updating the shower content depending on the emission corresponds to the shift operation in the quantum walk framework.

[†]Strictly speaking, the Hadamard coin introduces a bias to the quantum walk through the phase on the coin qubit. This is discussed in detail in [18] and references therein. Here we remove this bias by using a symmetric initial state.

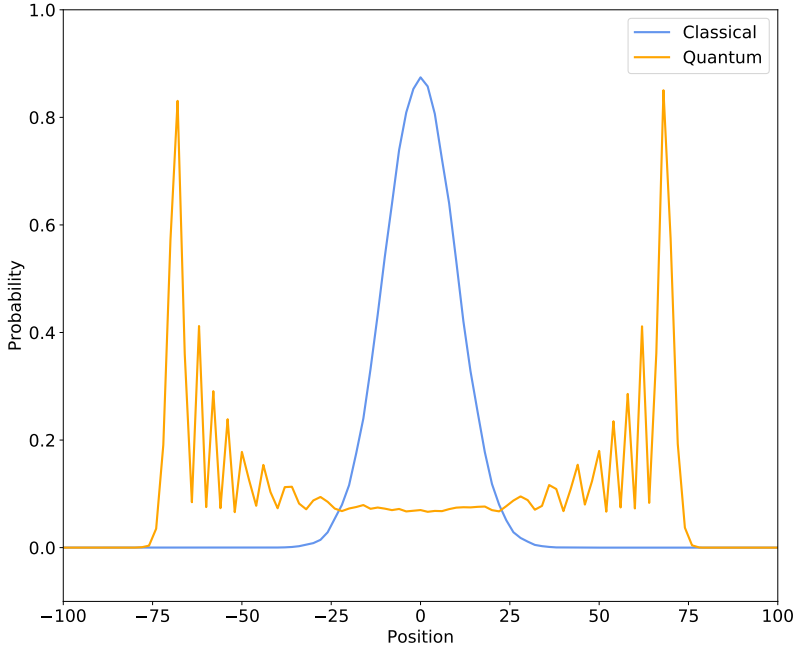


Figure 2: Simulation of a 100-step random walk using the IBM Q 32-qubit simulator [22] for 100,000 shots for a classical random walk obtained by measuring the coin state after each step, and a quantum random walk using a symmetric initial position and a Hadamard coin. Only non-zero probabilities are shown, as odd-numbered positions will have zero probability for this walk.

In this Section we detail this novel quantum walk approach to simulating a parton shower on a quantum device. Within this framework, the algorithm can simulate a many-particle parton shower, and shows a remarkable improvement on the number of shower steps that can be simulated in comparison to previous quantum algorithms [1, 2]. The Section is ordered as follows: Section 3.1 gives the theoretical outline of the toy model used in the parton shower, Section 3.2 shows the implementation of a simple parton shower with one particle type, Section 3.3 outlines the full collinear parton shower and Section 3.4 discusses possible extensions to the algorithm with advancements in quantum computers to simulate a realistic parton shower.

3.1 Theoretical outline of shower algorithm

We present a discrete, collinear parton shower using the quantum walk framework. As with the parton shower algorithms presented in [1, 2], this algorithm utilises the ability of the quantum device to remain in a superposition state throughout the calculation. Consequently, all shower histories are calculated simultaneously and are encoded in the final wavefunction, with a measurement projecting out a specific quantity of the final state, e.g.

the number of partons. This offers a unique advantage over classical parton shower algorithms, which need to calculate each shower history explicitly and store the information on a physical memory device. Only after summing over all possible shower histories can a physically meaningful quantity be extracted. The goal of this algorithm is to create the foundation for the development of a full, general parton shower by studying a simplified toy model that meets the capabilities of current quantum simulators.

An emission is collinear if a parton with momentum P splits into two massless particles, which have parallel 4-momenta, such that the momentum distribution is,

$$p_i = zP, \quad p_j = (1-z)P, \quad (3.1)$$

thus, $(p_i + p_j)^2 = P^2 = 0$ [24]. In this algorithm, we use a similar theoretical set-up as [2]. In each shower step, emission is determined by first ascertaining whether an emission occurred in the step using the Sudakov factors, and then applying the relevant splitting functions. The Sudakov factors for a QCD process are given by,

$$\Delta_{i,k}(z_1, z_2) = \exp \left[-\alpha_s^2 \int_{z_1}^{z_2} P_k(z') dz' \right], \quad (3.2)$$

and are used to calculate the probability of non-emission [25]. The probability that no particles split for an arbitrary step N in the shower process, where N particles can be present, is given by the total Sudakov factor,

$$\Delta_{\text{tot}}(z_1, z_2) = \Delta_g^{n_g}(z_1, z_2) \Delta_q^{n_q}(z_1, z_2) \Delta_{\bar{q}}^{n_{\bar{q}}}(z_1, z_2) \quad (3.3)$$

where n_g , n_q and $n_{\bar{q}}$ are the number of gluons, quarks and antiquarks present in the step[†]. As in [2], only collinear splittings will be considered. The emission probabilities are therefore calculated using the collinear splitting functions outlined in [26–28]. The emission of a gluon from a quark is defined at leading order (LO) by,

$$P_{q \rightarrow qg}(z) = C_F \frac{1 + (1-z)^2}{z}, \quad (3.4)$$

where $C_F = 4/3$ is calculated using colour algebra, and the quark and gluon have momentum fractions $1-z$ and z respectively. The gluon can self-couple, and therefore can split to both a pair of gluons and a quark-antiquark pair. At LO, the splitting functions for these emissions are,

$$P_{g \rightarrow gg}(z) = C_A \left[2 \frac{1-z}{z} + z(1-z) \right], \quad P_{g \rightarrow q\bar{q}}(z) = n_f T_R (z^2 + (1-z)^2), \quad (3.5)$$

where $C_A = 3$ and $T_R = 1/2$ are calculated using colour algebra, and n_f is the number of massless quark flavours.

[†]As the algorithm allows for steps with no emissions, for a step N : $(n_g + n_q + n_{\bar{q}}) \leq N$

Combining the Sudakov factors with the splitting functions defines the full probability of emission,

$$\text{Prob}_{k \rightarrow ij} = (1 - \Delta_k) \times P_{k \rightarrow ij}(z). \quad (3.6)$$

In the QW framework, this probability is applied as a unitary rotation to the coin qubit, defining the shower algorithm's coin operation.

The proposed algorithm does not include kinematics. This allows for the calculation to be implemented on currently accessible simulators, such as the 32-qubit IBM Q Quantum Simulator [22]. As a result, the shower evolution cannot be determined by the kinematics of the shower particles, but instead the evolution variable z is evolved to lower and lower momenta, exponentially with the number of steps. Section 3.4 outlines how a more realistic parton shower could be constructed on future devices.

3.2 Implementation of a simple shower as a one-dimensional quantum walk

The implementation of a parton shower as a quantum walk follows the framework of a simple quantum random walk outlined in Section 2. Here we define the coin operation as a unitary rotation on the coin qubit corresponding to the probability of emission, calculated using the Sudakov factors and the subsequent splitting functions defined in Section 3.1. This rotation takes the form,

$$U_c = \begin{pmatrix} \sqrt{1 - P_{jk}} & \sqrt{P_{jk}} \\ \sqrt{P_{jk}} & \sqrt{1 - P_{jk}} \end{pmatrix}, \quad (3.7)$$

where $P_{jk} = (1 - \Delta_i) \times P_{i \rightarrow jk}$ is the probability of particle i splitting to j and k . The coin space, \mathcal{H}_C , therefore spans the space $\{|0\rangle, |1\rangle\}$ defined by the possible measured states of the coin qubit. Here we define the $|0\rangle$ state as the “*no emission*” state, and the $|1\rangle$ state as the “*emission*” state. The position space, \mathcal{H}_P , now defines the number of particles present in the shower and has been altered to include only zero and positive integers, $\{|i\rangle : i \in \mathbb{N}_0\}$, as the parton shower cannot have a negative number of particles. The shift operation controls from the coin qubit and moves the walker in the correct direction. In order to apply the correct splitting probabilities to the coin qubit, the number of particles present must be determined. An efficient scheme has been created using a series of CNOT gates to determine the position of the walker.

To illustrate this simple shower, Figure 3 shows a schematic of a one-dimensional quantum walk able to simulate a particle which can split to produce another particle of the same type. In this simple shower, the number of particles present is encoded in the position of the walker. Figure 3 uses a two qubit basis for the position of the walker, ultimately allowing the algorithm to simulate a maximum of 4 shower particles in the final state. The number of particles that the algorithm can simulate increases exponentially with the number of position qubits, x , as 2^x . For this example, only one splitting is possible, $i \rightarrow ii$, and as a result only one coin qubit is needed to encode the splitting probability. If after the coin operation, the coin qubit is in the $|1\rangle$ state, then the splitting has occurred and the position of the walker is increased by one, thus increasing the number of particles

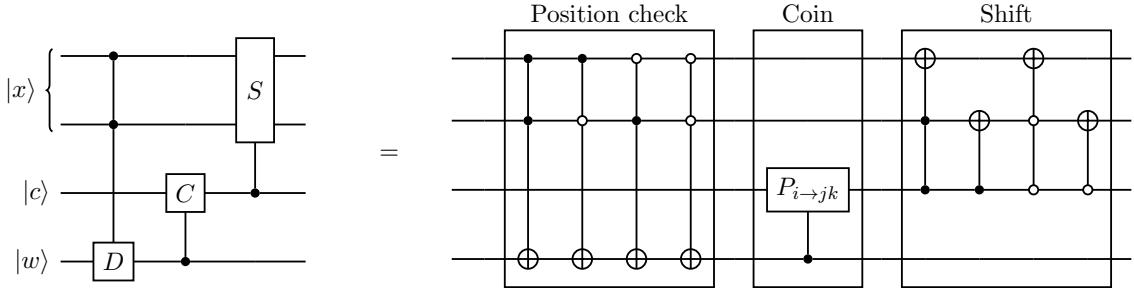


Figure 3: Template for a single step of a quantum walk as a parton shower, with the ability to simulate a particle which can split to more particles of the same type. Here, the “*position check*” determines the number of particles present by assessing the position of the walker. The “*coin*” operation applies the correct splitting probabilities depending on the position of the walker. The “*shift*” operation moves the walker depending on the outcome of the coin operation.

present in the shower by one. However, if the coin operation yields a $|0\rangle$ state, then the walker does not move for this simple example[§]. This step can then be repeated for the number of discrete shower steps in the parton shower, resembling the quantum random walk outlined in Section 2. Throughout the calculation, the device is in a superposition state of all possible outcomes of the coin and shift operations. At the end of the shower process, the final state of the system is measured and projected onto a classical state.

3.3 Implementation of a collinear parton shower

It is possible to extend the simple shower outlined in Section 3.2 to include multiple parton types by increasing the dimension of the position space \mathcal{H}_P , with the aim of developing a multi-particle, discrete, collinear parton shower using the theoretical outline discussed in Section 3.1. The algorithm presented here considers a toy model comprised of a gluon and one flavour of quark, and can simulate the corresponding splittings.

As shown in Section 3.2, a quantum walker in a one-dimensional position space, \mathcal{H}_P , has the ability to simulate a single particle type. Augmented by the coin space, \mathcal{H}_C , with dimension equal to the number of possible splittings associated with the particle, the quantum walk can simulate a simple parton shower comprising one particle type. Increasing the dimension of the position space increases the number of particles which can be simulated in the algorithm. Applying this mechanism to our toy model of the parton shower, the position space, \mathcal{H}_P , is increased to two dimensions to accommodate the simulation of gluons and quarks, counting gluons in one dimension and quarks in the other. Note that we do not need to include dimensions for both quarks and antiquarks as they are produced in conjunction through the $g \rightarrow q\bar{q}$ splitting, thus instead we count quark-antiquark pairs. Figure 4 shows a visualisation of how the walker’s position on a 2D plot corresponds to the number of particles in the shower, with gluons and quarks measured on the x and y -axes of

[§]Note that in Figure 3 the shift operation also shows the ability to decrease the walker’s position. This is not needed for the simple example of $i \rightarrow ii$ splittings, but will be useful later.

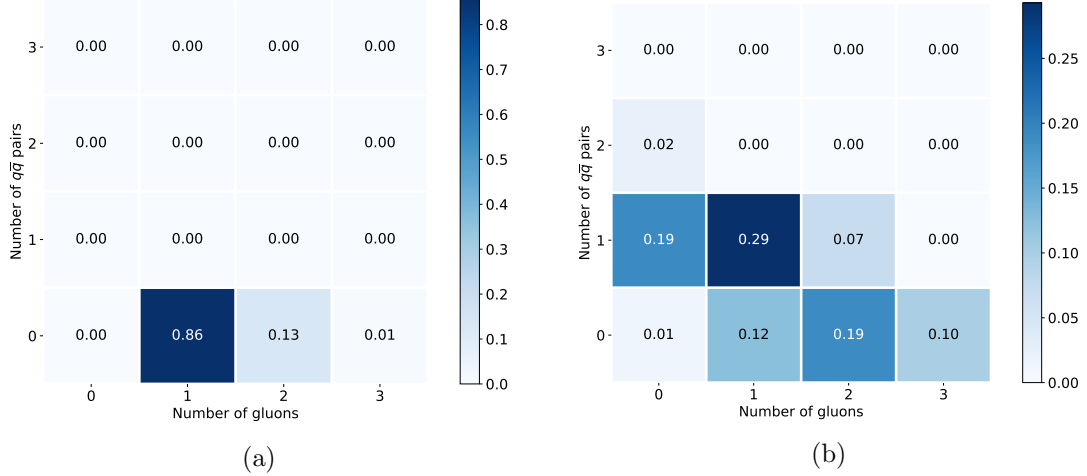


Figure 4: Visualisation of a quantum walk as a parton shower comprising gluons and quarks. The quantum walker's position on a 2D plot corresponds to the number of particles in the parton shower: (a) shows a parton shower using the collinear splitting functions for quarks and gluons, (b) shows a parton shower with modified splitting functions to show how the walker moves in the 2D lattice.

the walker's 2D lattice respectively. The coin space, \mathcal{H}_C , is increased to a three-dimensional Hilbert space, with three coin qubit rotations corresponding to the splitting functions in Equations 3.4 and 3.5. Controlled from the coin register, the shift operations propagate the walker to reflect the production of new particles in the shower step. A schematic of the quantum circuit is shown in Figure 5. It should be noted that it is likely that more than one of the coin qubits can be in the $|1\rangle$ state in a step. In these situations, it is not clear which splitting kernel should be applied and therefore the algorithm does not apply a shift operation to the walker. This is realised by controlling from coin states that only have one coin qubit in the $|1\rangle$ state, as shown in Figure 5.

To simulate a parton shower, the steps shown in Figure 5 are performed many times, with only one splitting allowed to occur per step. Steps where no emission occurred are dictated by the Sudakov form factors from Equation 3.3. The system is kept in a superposition state throughout the algorithm, with a measurement taking place only at the end of the calculation. Therefore, after all the steps have been evaluated, the system is in a superposition of all possible shower histories. This differs dramatically from classical parton shower algorithms where each shower history must be individually calculated. A physically meaningful quantity can only be extracted from a classical shower algorithm once all possible shower histories have been summed over. Consequently, the quantum algorithm approach to parton showers provides a unique advantage over the classical approach.

The quantum parton shower algorithm with 31 shower steps has been run for 500,000 shots on the IBM Q 32-qubit Quantum Simulator [22]. The output from the quantum simulator has been compared to a classical parton shower algorithm, which follows the same theoretical framework as that outlined in Section 3.1, simulating a toy model with

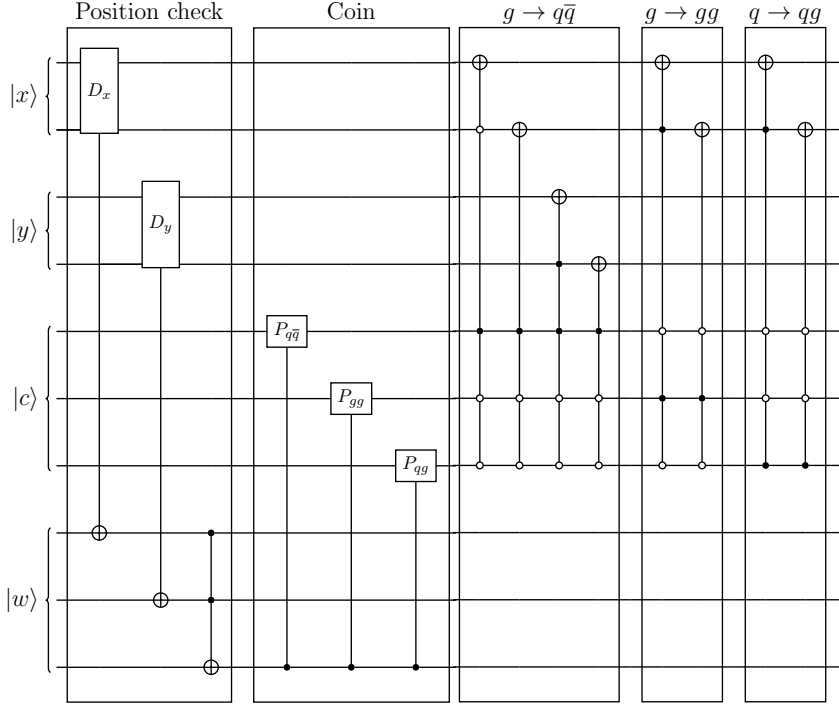


Figure 5: Schematic of the quantum circuit for a single step of a discrete QCD, collinear parton shower with the ability to simulate the splittings of gluons and one flavour of quark. The shower algorithm is split into 3 distinct sections: (1) The position check determines the position of the walker so that the correct Sudakov form factors are applied in the splitting kernels, (2) the coin flip applies unitary rotations to a coin register corresponding to the possible splitting kernels, (3) the shift operation propagates the walker into correct direction to describe the particle splitting in the shower step. This step is then repeated iteratively to simulate a full shower process.

one quark flavour and a gluon. Figure 6 shows the comparison between the quantum and classical parton shower algorithms of the probability distributions of the number of gluons measured at the end of the shower. This is shown for the scenario where there are zero quark-antiquark pairs in the final state and the much less probable scenario where there is one quark-antiquark pair in the final state. Due to the low statistics for the $1q\bar{q}$ results, a further validation of the parton shower algorithm has been carried out using modified splitting functions to enhance the $g \rightarrow q\bar{q}$ and $q \rightarrow qg$ splittings. The results of this test are shown in Figure 7 and display good agreement between the quantum and classical parton shower algorithms. The probability of producing two quark-antiquark pairs is less than 10^{-5} . For both comparison runs, the classical algorithm has been executed for 31 shower steps with 10^6 shots of the algorithm.

The algorithm is implemented using 16 qubits to simulate a parton shower of 31 steps. This is a dramatic increase in the number of steps that can be simulated on a quantum device in comparison to previous algorithms [1, 2], with almost a factor of two reduction in the number of required qubits [2].

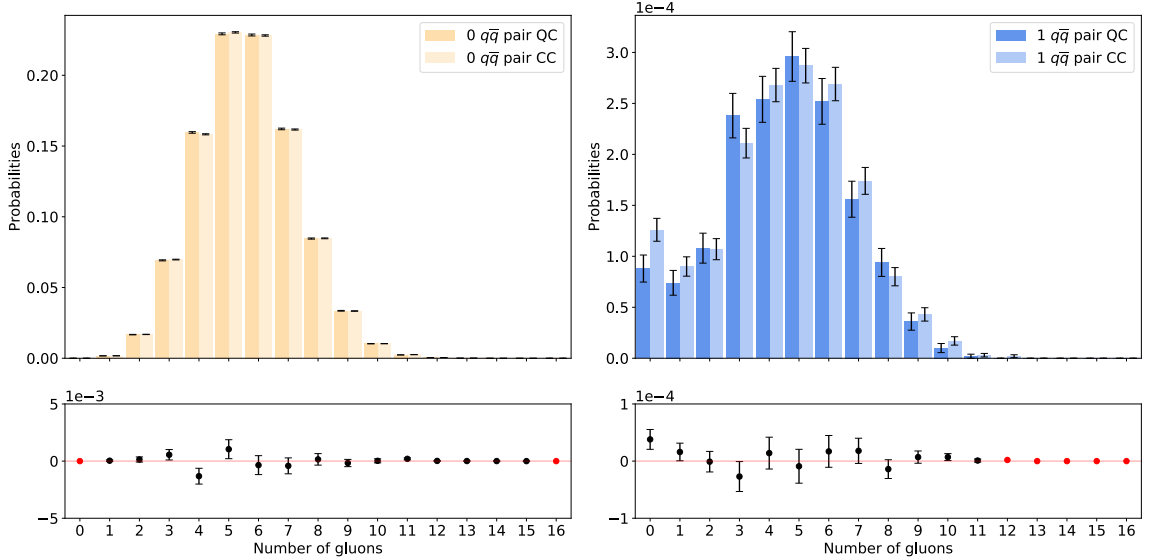


Figure 6: Probability distribution of the number of gluons measured at the end of the 31-step parton shower for the classical and quantum algorithms, for the scenario where there are zero quark anti-quark pairs (left) and exactly one quark anti-quark pair (right) in the final state. The quantum algorithm has been run on the IBMQ 32-qubit quantum simulator [22] for 500,000 shots, and the classical algorithm has been run for 10^6 shots.

3.4 Towards a realistic parton shower

The parton shower algorithm described in Section 3.3 is a simplified, toy model and has thus limited capability compared to state-of-the-art, classical parton shower algorithms. However, the quantum algorithm leverages the unique ability of the quantum computer to remain in a superposition state throughout the calculation, enabling all shower histories to be calculated simultaneously and providing a remarkable advantage over the classical algorithms. It is interesting to consider how the parton shower algorithm will develop with advancements in quantum technologies. Near-future devices with larger quantum volume [29, 30] make it feasible to imagine a practical parton shower algorithm on a quantum device.

An obvious extension to the algorithm proposed would be to include more particle types and flavours. As described in Section 3.3, this is easily done by increasing the dimension of the \mathcal{H}_P and \mathcal{H}_C spaces to include another particle and its corresponding splittings. It may then be possible to extend the shower to include all quark flavours, increasing the dimension of the walker's lattice to seven: six quark dimensions and one gluon dimension. To implement this circuit would require a large number of qubits, with the number required for each particle type being

$$n_{\text{qubits}} = \log_2 N, \quad (3.8)$$

where N is the number of desired steps in the shower process. It is possible to reduce the overall number of qubits in the system by removing redundant areas in the quantum

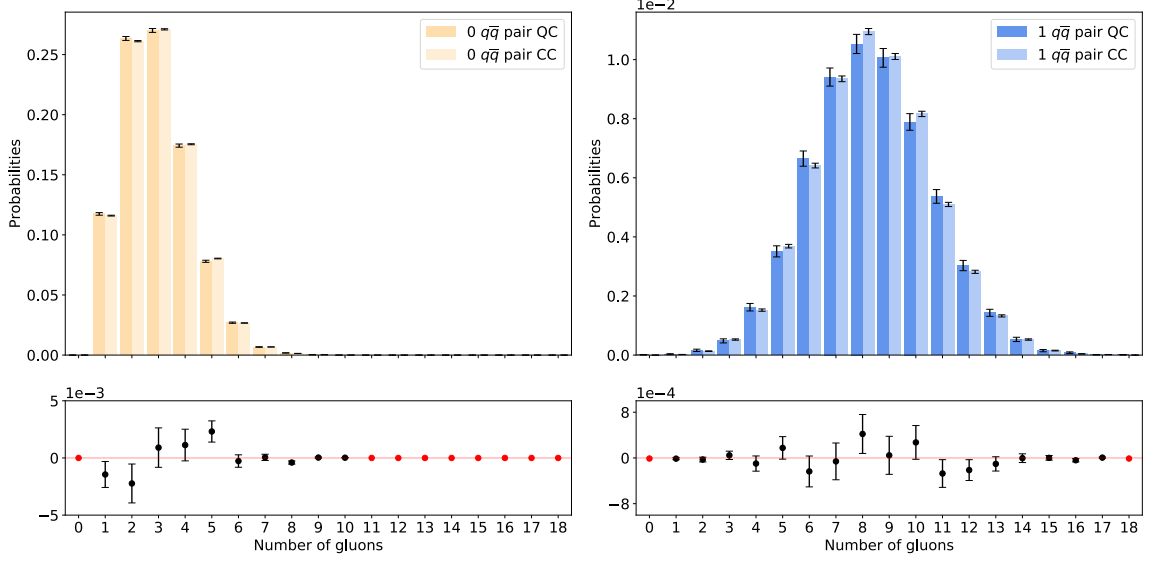


Figure 7: Probability distribution of the number of gluons measured at the end of the 31-step parton shower for the classical and quantum algorithms with modified splitting kernels, for the scenario where there are zero quark anti-quark pairs (left) and exactly one quark anti-quark pair (right) in the final state. The quantum algorithm has been run on the IBMQ 32-qubit quantum simulator [22] for 100,000 shots, and the classical algorithm has been run for 10^6 shots.

walker's lattice. For example, in Figures 6 and 7, there is only one quark-antiquark pair in the results. Therefore, all lattice sites containing two or more quark-antiquark pairs could be removed to streamline the circuit. However, this does reduce the generality of the circuit, and such areas would have to be known a priori to running the device.

It is feasible to consider an algorithm that can simulate a parton shower for calculations where a basis transformation is performed. For example, in [1] a parton shower algorithm was proposed with two fermions f_1 and f_2 and a scalar ϕ . The algorithm considers a rotation from the flavour basis, $f_{1/2}$, to a mass basis, $f_{a/b}$. The parton shower calculation is then carried out in the mass basis, rotating back to the flavour basis before measurement. It claims an advantage over classical algorithms by simulating the quantum interference between the two fermions. Due to the qubit requirement of the circuit, the full algorithm was restricted to 2 steps in the shower process. It is possible to replicate the parton shower algorithm from [1] in a quantum walk framework by increasing the dimension of the position space \mathcal{H}_P and the coin space \mathcal{H}_C to include the two fermions and one scalar, and their corresponding splitting functions. The basis transformation can be reproduced as a rotation across the fermion dimensions of the position space \mathcal{H}_C . The shower would then follow the quantum walk process outlined in Equation 2.3, with a final rotation across the fermion position space to transform back to the flavour basis before measurement. This algorithm would be able to run for many steps and would be a good test of the quantum advantage claimed in [1].

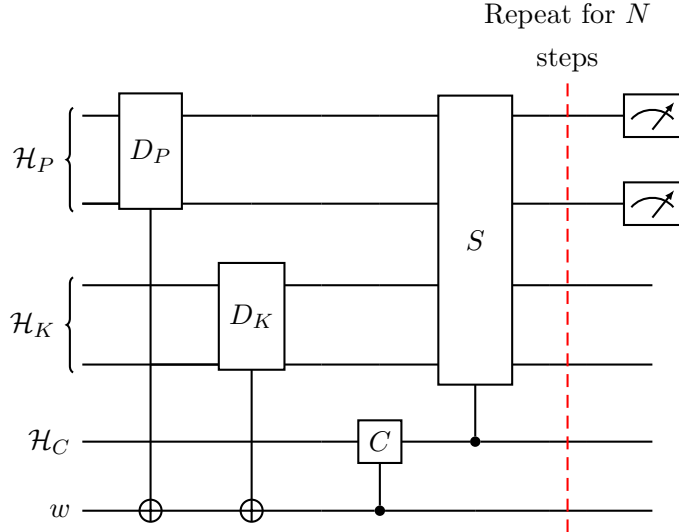


Figure 8: A schematic circuit diagram for a one particle type parton shower with a discretised kinematic space. Here, \mathcal{H}_P , \mathcal{H}_K and \mathcal{H}_C are the position, kinematic and coin spaces respectively, and w is an ancillary register.

Keeping track of particle kinematics in the parton shower algorithm outlined in Section 3.3 is an important step towards emulating a realistic parton shower. The current publicly accessible devices and simulators do not have adequate quantum volume to include shower kinematics, but future devices may have the capability to implement this. Within the quantum walk framework, it is possible to consider extending the Hilbert space of the system to include a *kinematic* space \mathcal{H}_K such that the total space now has the form,

$$\mathcal{H} = \mathcal{H}_C \otimes \mathcal{H}_P \otimes \mathcal{H}_K. \quad (3.9)$$

The kinematic space \mathcal{H}_K would comprise a discretised momentum space that each shower particle could move in. Similarly to the position check in Figure 5, conditional coin operations would then be used to apply the correct splitting kernels to the coin qubits depending on the position of the walker in the kinematic space \mathcal{H}_K . A schematic of a one particle type parton shower, with kinematics included, is shown in Figure 8. It should be noted that, in order to keep track of each particle's momentum in the shower, the kinematic space \mathcal{H}_K will have to be extended at each splitting. One can initialise the system to have the whole kinematic space at the beginning of the algorithm, populating the space only in the event of a splitting. However, this approach will lead to a large redundancy in the circuit, an area which may have to be optimised in practice.

4 Summary

Simulating parton showers on quantum computers has been shown [1, 2] to have distinct advantages that exploit the unique features of the quantum device. In classical parton showers, all possible shower histories are calculated individually, stored on a physical memory

device and then analysed in their entirety to provide information on a physical quantity. In contrast, the quantum device remains in a quantum state throughout the calculation, constructing a wavefunction which comprises a superposition of all possible shower histories. Consequently, all shower histories are calculated simultaneously in a single calculation, removing the requirement to store and track each shower history on physical memory. However, simply porting over the classical parton shower implementations onto a quantum device is computationally inefficient, requiring a large number of qubits and only allowing up to 2 steps of the parton shower to be simulated on current simulators [2].

This paper proposes a novel quantum walk approach to simulating parton showers on a quantum computer that represents a significant improvement in the depths of the shower that can be simulated and with far fewer qubits. We present a quantum algorithm for the simulation of a collinear, 31-step parton shower implemented as a 2D quantum walk, where the coin flip represents the total parton emission probability, and the movement of the walker in the 2D space represents an emission corresponding to either gluons or a quark-antiquark pair. Reframing the parton shower in this quantum walk paradigm enables a 31-step shower to be simulated, a dramatic improvement over previous quantum algorithms [1, 2] and with almost a factor of two reduction in the number of required qubits [2]. The quantum walk approach thus offers a natural and much more efficient approach to simulating parton showers on quantum devices. Furthermore, the algorithm scales efficiently: the number of possible shower steps increase exponentially with the number of qubits in the position registers; and the circuit depth grows linearly with the number of steps, in contrast to previous algorithms which grow quadratically, at best.

Acknowledgements: *Sarah Malik and Simon Williams are funded by grants from the Royal Society. We would like to acknowledge the use of the IBM Q for this work. We thank Frank Krauss and Stefan Prestel for valuable discussions.*

References

- [1] C. W. Bauer, W. A. de Jong, B. Nachman, and D. ide Provasoli, *A quantum algorithm for high energy physics simulations*, 2019.
- [2] K. Bepari, S. Malik, M. Spannowsky, and S. Williams, *Towards a quantum computing algorithm for helicity amplitudes and parton showers*, *Phys. Rev. D* **103** (Apr, 2021) 076020.
- [3] T. Li, X. Guo, W. K. Lai, X. Liu, E. Wang, H. Xing, D.-B. Zhang, and S.-L. Zhu, *Partonic structure by quantum computing*, 2021.
- [4] S. Das, A. J. Wildridge, S. B. Vaidya, and A. Jung, *Track clustering with a quantum annealer for primary vertex reconstruction at hadron colliders*, 2020.
- [5] C. Tüysüz, F. Carminati, B. Demirköz, D. Dobos, F. Fracas, K. Novotny, K. Potamianos, S. Vallecorsa, and J.-R. Vlimant, *Particle track reconstruction with quantum algorithms*, *EPJ Web of Conferences* **245** (2020) 09013.
- [6] D. Magano, A. Kumar, M. Kālis, A. Locāns, A. Glos, S. Pratapsi, G. Quinta, M. Dimitrijevs,

- A. Rivošs, P. Bargassa, J. Seixas, A. Ambainis, and Y. Omar, *Quantum speedup for track reconstruction in particle accelerators*, 2021.
- [7] A. Blance and M. Spannowsky, *Quantum Machine Learning for Particle Physics using a Variational Quantum Classifier*, [[arXiv:2010.07335](https://arxiv.org/abs/2010.07335)].
 - [8] A. Blance and M. Spannowsky, *Unsupervised Event Classification with Graphs on Classical and Photonic Quantum Computers*, [[arXiv:2103.03897](https://arxiv.org/abs/2103.03897)].
 - [9] K. Terashi, M. Kaneda, T. Kishimoto, M. Saito, R. Sawada, and J. Tanaka, *Event classification with quantum machine learning in high-energy physics*, *Computing and Software for Big Science* **5** (Jan, 2021).
 - [10] S. L. Wu, J. Chan, W. Guan, S. Sun, A. Wang, C. Zhou, M. Livny, F. Carminati, A. Di Meglio, A. C. Y. Li, and et al., *Application of quantum machine learning using the quantum variational classifier method to high energy physics analysis at the lhc on ibm quantum computer simulator and hardware with 10 qubits*, *Journal of Physics G: Nuclear and Particle Physics* (Jul, 2021).
 - [11] J. Y. Araz and M. Spannowsky, *Quantum-inspired event reconstruction with Tensor Networks: Matrix Product States*, *JHEP* **08** (2021) 112, [[arXiv:2106.08334](https://arxiv.org/abs/2106.08334)].
 - [12] V. Belis, S. González-Castillo, C. Reissel, S. Vallecorsa, E. F. Combarro, G. Dissertori, and F. Reiter, *Higgs analysis with quantum classifiers*, *EPJ Web of Conferences* **251** (2021) 03070.
 - [13] A. E. Armenakas and O. K. Baker, *Application of a quantum search algorithm to high-energy physics data at the large hadron collider*, 2020.
 - [14] D. Pires, P. Bargassa, J. Seixas, and Y. Omar, *A digital quantum algorithm for jet clustering in high-energy physics*, 2021.
 - [15] A. Mott, J. Job, J.-R. Vlimant, . D. Lidar, and M. Spiropulu, *Solving a higgs optimization problem with quantum annealing for machine learning*, *Nature* **550** (10, 2017) 375–379.
 - [16] Y. Aharonov, L. Davidovich, and N. Zagury, *Quantum random walks*, *Phys. Rev. A* **48** (Aug, 1993) 1687–1690.
 - [17] D. Aharonov, A. Ambainis, J. Kempe, and U. Vazirani, *Quantum walks on graphs*, *Conference Proceedings of the Annual ACM Symposium on Theory of Computing* (01, 2001).
 - [18] J. Kempe, *Quantum random walks: An introductory overview*, *Contemporary Physics* **44** (2003), no. 4 307–327, [<https://doi.org/10.1080/00107151031000110776>].
 - [19] P. Rohde, A. Schreiber, M. Štefaňák, I. Jex, A. Gilchrist, and C. Silberhorn, *Increasing the dimensionality of quantum walks using multiple walkers*, *Journal of Computational and Theoretical Nanoscience* **10** (2012) 1644–1652.
 - [20] IBM Research, *Qiskit, an open source computing framework*, .
 - [21] A. Ambainis, E. Bach, A. Nayak, A. Vishwanath, and J. Watrous, *One-dimensional quantum walks*, (New York, NY, USA), Association for Computing Machinery, 2001.
 - [22] IBM Q Team, *IBM Q 32 Simulator v0.1.547*, .
 - [23] A. Buckley *et. al.*, *General-purpose event generators for LHC physics*, *Phys. Rept.* **504** (2011) 145–233, [[arXiv:1101.2599](https://arxiv.org/abs/1101.2599)].
 - [24] T. R. Taylor, *A course in amplitudes*, *Physics Reports* **691** (May, 2017) 1–37.

- [25] V. Sudakov, *Vertex parts at very high-energies in quantum electrodynamics*, Sov. Phys. JETP **3** (1956) 65–71.
- [26] Y. L. Dokshitzer, *Calculation of the Structure Functions for Deep Inelastic Scattering and $e+e-$ Annihilation by Perturbation Theory in Quantum Chromodynamics.*, Sov. Phys. JETP **46** (1977) 641–653.
- [27] V. Gribov and L. Lipatov, *Deep inelastic $e p$ scattering in perturbation theory*, Sov. J. Nucl. Phys. **15** (1972) 438–450.
- [28] G. Altarelli and G. Parisi, *Asymptotic freedom in parton language*, Nuclear Physics B **126** (1977), no. 2 298 – 318.
- [29] J. Gambetta, *Ibm's roadmap for scaling quantum technology*, Sep, 2020.
- [30] P. Jurcevic, A. Javadi-Abhari, L. Bishop, I. Lauer, D. F. Bogorin, M. Brink, L. Capelluto, O. Gunluk, T. Itoko, N. Kanazawa, A. Kandala, G. Keefe, K. D. Krsulich, W. Landers, E. P. Lewandowski, D. McClure, G. Nannicini, A. Narasgond, H. Nayfeh, E. Pritchett, M. B. Rothwell, S. Srinivasan, N. Sundaresan, C. Wang, K. X. Wei, C. Wood, J.-B. Yau, E. Zhang, O. Dial, J. Chow, and J. Gambetta, *Demonstration of quantum volume 64 on a superconducting quantum computing system*, 2020.